2014

Reduced residual stress curvature and branched comb fingers increase sensitivity of MEMS acoustic sensor

Downey, Richard H.; Karunasiri, Gamani

IEEE

Downey, Richard H., and Gamani Karunasiri. "Reduced residual stress curvature and branched comb fingers increase sensitivity of MEMS acoustic sensor." Journal of Microelectromechanical Systems 23.2 (2014): 417-423.
http://hdl.handle.net/10945/60329

Reduced Residual Stress Curvature and Branched Comb Fingers Increase Sensitivity of MEMS Acoustic Sensor

Richard H. Downey and Gamani Karunasiri

***Abstract*— We present an enhanced in-plane capacitive readout for sensing out-of-plane displacement in a MEMS acoustic sensor. The sensor is fabricated in a multi-user silicon-on-insulator process, using a thicker device layer to reduce misalignment between moving and fixed comb fingers. This misalignment is found to reduce the sensitivity and render the response nonlinear. In addition, incorporation of a branched comb design doubles the readout capacitor surface area for a given sensor size, to further increase the sensitivity. These two modifications restore linearity to the readout and increase its sensitivity to displacement by an order of magnitude. [2013-0191]**

***Index Terms*— Acoustic, MEMS, Sound sensor, capacitive readout.**

I. Introduction

CAPACITIVE comb fingers are commonly used for sensing displacement in MEMS devices. Typically the motion to be sensed is in the plane of the device, but it is also possible to use a comb finger capacitor to sense motion out of the plane [1]–[3]. One example of such an application is in an acoustic sensor inspired by the ear of the fly *Ormia ochracea* [4]–[6] with the goal of sensing the incidence direction of sounds [7], [8]. This sensor consists of a pair of relatively large wings that vibrate out of the device plane in response to sound. The wings are mechanically coupled by a narrow bridge, which is suspended from the substrate by two small legs at its center as shown in Fig. 1. This arrangement allows the wings to resonantly vibrate in two modes, in phase (bending) and out of phase (rocking), with characteristic frequencies determined by the spring constants of the bridge and legs, respectively [7], [9]. The amplitude of the rocking mode is relatively small compared to the bending mode since it is excited by the sound pressure difference between the wings, whereas the bending mode is excited by the total pressure [4]. The substrate beneath the wings and bridge is removed to allow the vertical motion, which is read out by comb finger capacitors on the wings. The open back configuration of the sensor allows sound to interact with both front and back of the wings resulting in direction sensing capability similar to pressure gradient microphones [10]. A commercially available MS3110 Universal Capacitive Readout integrated circuit converts the changes in comb finger capacitance to an output voltage ranging from 0–5 V. Accurate directional acoustic sensing depends on precisely measuring the vibration amplitude.

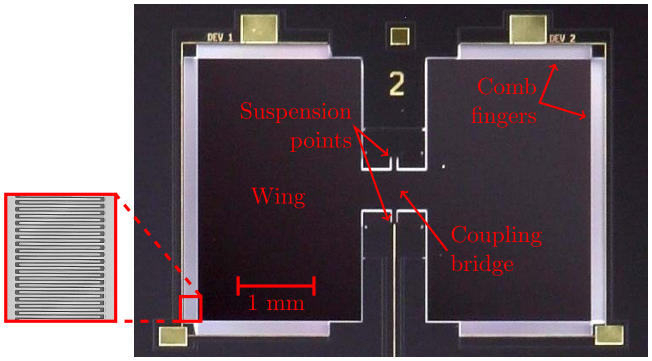

Fig. 1. The MEMS acoustic direction-finding sensor with straight comb fingers. The inset shows a scanning electron microscope (SEM) image of the comb fingers, which are 100 μm long. This is the sensor referred to as Sensor A.

The output voltage under sound excitation depends on the combined length or perimeter of the comb finger capacitors. This should be as long as possible, but the fabrication process constrains the length of the comb fingers, and the number of fingers is limited by the perimeter of the sensor wing. In our case, using the Silicon-On-Insulator Multi-User Process (SOIMUMPs [11]), features narrower than 6 μm should be no longer than 100 μm, and the smallest allowed feature size is 2 μm. This means the comb fingers can be no closer together than one opposing pair every 8 μm.

Figure 1 shows a sensor, referred to as Sensor A, fabricated using a 10 μm device layer, with dimensions chosen to have frequency response around 2 kHz. Our initial goal was simply to alter this design to increase the number of combs without making the sensor wing excessively large. However, while viewing Sensor A under an optical microscope, we found that the fingers on the wings were vertically displaced relative to the opposing fingers attached to the substrate. In addition to number of comb fingers, it is important that the moving and fixed fingers have good overlap to increase total capacitance as well as to achieve linear response. Further measurements

Manuscript received June 13, 2013; accepted August 5, 2013. Date of publication September 11, 2013; date of current version March 31, 2014. This work was supported by a National Consortium for MASINT Research grant. The work of R. H. Downey was supported by a U.S. Navy Space and Naval Warfare Systems Command Fellowship. Subject Editor N. F. de Rooij.

The authors are with the Department of Physics, Naval Postgraduate School, Monterey, CA 93943 USA (e-mail: rhd@alum.mit.edu; karunasiri@nps.edu).

Color versions of one or more of the figures in this paper are available online at http://ieeexplore.ieee.org.

Digital Object Identifier 10.1109/JMEMS.2013.2279017

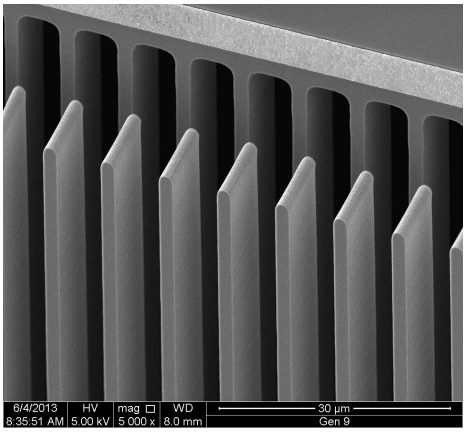

Fig. 2. Misaligned comb fingers in Sensor A.

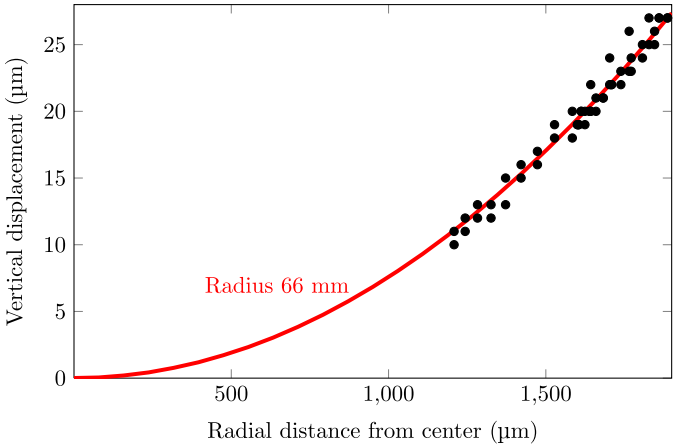

Fig. 3. Measured vertical displacement of Sensor A as a function of distance from the center (bold circles). The red curve shows an arc of a circle passing through the origin with radius 66 μm.

showed that the vertical displacement was greater than the thickness of the comb fingers, so that the opposing comb fingers were in fact not overlapped at all (see Fig. 2). The main reason for the misalignment is residual stress in the wings from the fabrication process.

In this paper, we show how the misaligned comb fingers reduced the readout sensitivity and introduced nonlinearity in the response, and describe an approach to achieve the proper alignment. The sensor fabricated using this approach shows a tenfold increase in sensitivity.

II. Comb Finger Misalignment

There are three important questions about the comb finger misalignment in Sensor A. First, what is its magnitude? Second, how does it affect the readout sensitivity? And third, how can it be corrected?

To address the first question, we measured the equilibrium vertical displacement z_0 of the comb fingers. This was done using an optical microscope with a 100× objective lens. First the fixed fingers attached to the substrate were brought into focus, and the fine focus knob setting was recorded. Next, the fingers attached to the sensor wing were brought into focus, and the setting was again recorded. The vertical displacement was measured to the nearest micron using the difference in focus settings. This process was repeated at intervals all the way around the sensor wing. At each position, the x and y coordinates relative to the sensor's center were recorded. Finally, the radial distance from the center was computed as $\rho = \sqrt{x^2 + y^2}$. This distance ranged from about 1200–1900 μm, and the vertical displacement $z_0(\rho)$ ranged from 10–27 μm, with an average of 20 μm and a standard deviation of 5 μm. These measured data are shown in Fig. 3, and are overlaid with a circle of radius 66 μm passing through the origin. Figure 3 clearly shows the circular nature of the vertical displacement $z_0(\rho)$, which indicates that the sensor curvature has spherical form. Analysis of similar observations, on this sensor and others fabricated using the same process, suggested that the radius of curvature R can be estimated from the device layer thickness t using the rule of thumb

$$R = t^2/1.4, \tag{1}$$

where R is expressed in millimeters and t in microns [8].

The second question about the misalignment is how it affects the readout sensitivity. Clearly the capacitors do not function as intended. As designed, the comb fingers should function as parallel plates of length l (combined length of all comb fingers), vertical height t (the device layer thickness), and capacitor gap d. The vertical displacement z varies, but the gap remains constant as long as $z < t$. In this ideal model, the capacitance per unit length is directly proportional to the comb overlap $t - z$:

$$\frac{C(z)}{l} = \frac{\epsilon_0 (t - z)}{d}, \tag{2}$$

in SI units, where $\epsilon_0 = 8.85$ pF/m. A vibration of amplitude Δz produces a capacitance amplitude (per unit length) given by the derivative of this expression, so that

$$\left| \frac{\Delta C}{l} \right| = \frac{\epsilon_0}{d} |\Delta z|. \tag{3}$$

Because the readout circuit converts changes in capacitance linearly to voltage amplitude, the output voltage should also vary linearly with vibration amplitude. Also, note that the equilibrium displacement z_0 does not affect the output, since only Δz appears in Eq. (3).

However, when the comb fingers on the wing are displaced by an equilibrium distance $z_0 > t$ as illustrated in Fig. 4, the model described earlier breaks down. Now the displaced comb fingers act together as the upper "plate" of a new horizontally aligned capacitor, while the non-displaced comb fingers act as the lower plate (see Fig. 4). These plates include a considerable amount of empty space due to gaps between fingers, but nevertheless still function as a parallel plate capacitor, like the diaphragm and backplate capacitors commonly used in microphones. In this configuration, it is the gap between plates that varies with vibration. Thus, the change in capacitance is nonlinear since the gap appears in the denominator. Specifically, if the comb finger width is w and the combined length is again l, then the area of each plate

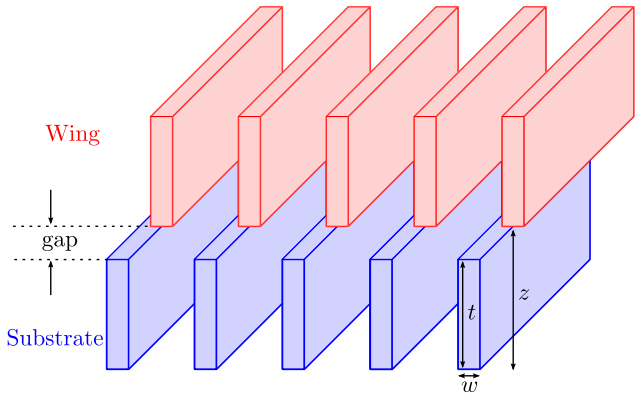

Fig. 4. When the comb fingers are misaligned, the wing (moving) comb and the substrate (fixed) comb act as the two plates of a horizontal capacitor.

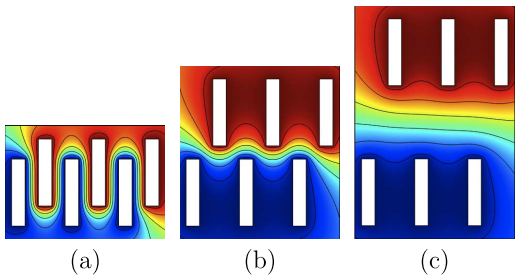

Fig. 5. The finite element model of capacitance per unit length. The white rectangles are the comb finger cross-sections. The color scale represents the electric potential, and equipotential lines are drawn in black.

is wl, and the capacitance is

$$\frac{C(z)}{l} = \frac{\epsilon_0 w}{z - t}. \tag{4}$$

Eq. (4) indicates that the capacitance changes nonlinearly with the location z of the moving wing. During the part of the oscillation where the gap $z - t$ is very small, the changes in capacitance are much larger than elsewhere in the cycle. It is this part of the cycle that contributes most to the nonlinearity.

To validate the two analytical models for the capacitance of aligned and misaligned comb fingers, a two-dimensional finite element model (FEM) was created using COMSOL MULTIPHYSICS 4.3 software. The FEM simulated a vertical cross section of a bank of comb fingers of width $w = 2$ μm and height $t = 10$ μm, with every second finger displaced vertically a variable distance z. The displaced fingers represented those attached to the sensor wing, while the non-displaced fingers represented those fixed to the substrate. In this simulation, z can be less than or greater than t. During the simulation, a positive voltage was applied to the moving fingers, and a negative voltage to the fixed fingers; the software computed the resulting electric potential everywhere and automatically returned the capacitance per unit length. Plots of the electric potential for three different values of z are shown in Fig. 5.

In Fig. 5a, where $z < t$, the comb fingers perform as intended. Equipotential lines are between the fingers and parallel, indicating that the capacitance should decrease linearly

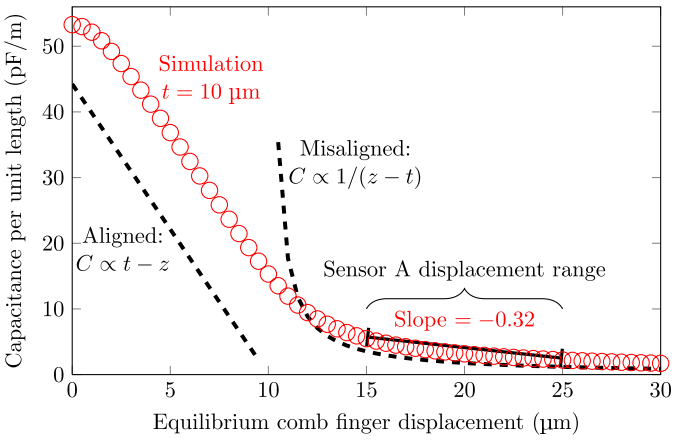

Fig. 6. Simulated capacitance per unit length of a comb finger bank with $t = 10$ μm, as a function of vertical displacement z. Dashed lines show the analytical models for aligned ($z < t$) and misaligned ($z > t$) comb fingers.

with z. In Fig. 5b, where $z \sim t$, the equipotentials are wavy, indicating that it would be difficult to develop a good analytical model for values of z in this region. Finally, in Fig. 5c, where $z \gg t$, the equipotentials are again reasonably straight but now horizontal. This indicates that the two-plate model for vertically misaligned comb fingers should be reasonably accurate for values of z in this region.

The z-dependence of the capacitance per unit length was modeled by repeating this simulation for a series of values of z. The simulated values of $C(z)/l$ for Sensor A are shown in Fig. 6, along with the analytical models for both aligned and misaligned comb fingers. From Fig. 6, it is clear that the two-plate model is reasonably accurate in the range of displacements obtained by Sensor A. It will be noted that the idealized model (for properly aligned fingers) clearly underestimates the capacitance compared to the simulation results. This is due to the fringing effects at the capacitor edges, which are significant when the capacitor plates are only a few times larger than the gap (2 μm) between them. However, the simulation suggests that the fringing does not much affect the *slope* of $C(z)/l$. Since the output voltage is determined by this slope, the fringing effects do not play an important role.

Note that the simulated capacitance slope decreases as z goes to zero. This indicates that the fringing effect is not entirely constant. The significance is that nonzero equilibrium displacement is actually desirable, because the steepest capacitance slope occurs not at $z = 0$, but at values of z between about 2 μm and the device layer thickness. This wide range of maximum sensitivity is convenient since the residual stress curvature causes the equilibrium comb finger displacement to vary around the wing. As long as all comb fingers are displaced somewhere within this range, the output voltage will be maximized and linearly proportional to the vibration amplitude.

The final question about the comb finger misalignment is how it can be corrected. There are many ways to reduce the curvature due to residual stress in MEMS devices, but the SOIMUMPs process offers very limited options. The

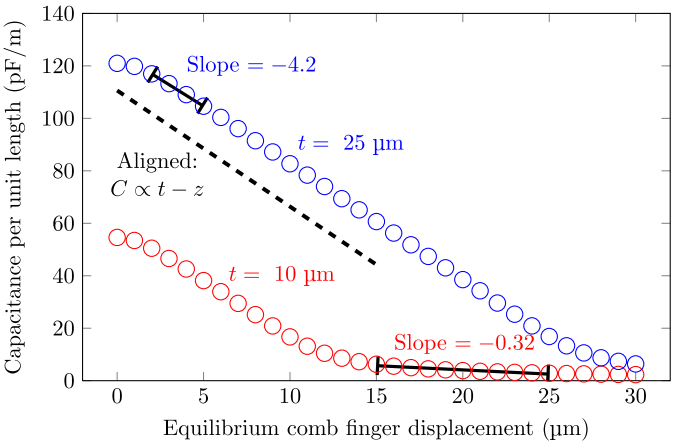

Fig. 7. Simulated capacitance per unit length as a function of comb finger vertical displacement z. The black lines represent the average displacement for Sensors A and B, and the sensitivity to vibration is proportional to the slope of these lines.

only layers available are the substrate wafer, the insulating oxide layer, the single-crystal silicon device layer, and two metal layers. There is no ability to partially etch any layers; each layer is patterned at full thickness or not at all. Because the upper part of the single-crystal silicon device layer is heavily doped to increase conductivity [11], the residual stress is inherent in the process. However, there is one way to reduce the effect of this stress, namely a choice of silicon device layer thickness of either 10 μm or 25 μm. According to Eq. (1), the wing curvature radius varies as the square of the device layer thickness. Thus, the thicker device layer should produce a sensor with significantly less curvature.

To confirm that a sensor with thicker device layer (Sensor B) should have improved readout sensitivity, the computer simulation was repeated for comb fingers 25 μm thick. The results are plotted in Fig. 7 along with the previous results from the 10 μm simulation. The 25 μm simulation shows that the slope in the range $z < t$ is again essentially the same as the analytical model. The equilibrium comb finger displacement ranges for both sensors (measured in the case of Sensor A, predicted for Sensor B) are indicated by black lines, along with the capacitance slopes in those ranges. Keeping in mind that the output voltage amplitude is directly proportional to the change in capacitance during vibration under sound excitation, the ratio of these slopes suggests that Sensor B should be approximately 13 times as sensitive to vibration as Sensor A.

III. The Sensor B Design

Designing a sensor using the 25 μm device layer posed one significant challenge due to the greater stiffness associated with the higher thickness. Specifically, the sensor outline had to be changed to keep the resonant frequencies close to those of the Sensor A. The operating frequency ω_0 for the bending mode is determined by the wing mass m and coupling bridge stiffness k, through the relationship $\omega_0 = \sqrt{k/m}$. Since the bridge acts as a fixed-free cantilever beam, the stiffness is proportional to thickness cubed but inversely proportional to the bridge length cubed [9]. Clearly, the mass increases only linearly with thickness, and thus a thicker sensor has a higher bending frequency, all other things being equal.

To keep the resonant frequencies roughly the same as in Sensor A, the coupling bridge in the Sensor B was made narrower, and was extended into the wings to make it longer without increasing the overall sensor size. Also, the mass of Sensor B was increased by incorporating both of the two available metal layers on the wing surface, which resulted in a combined metal thickness of 1.2 μm [11]. Finally, Sensor B was given the branched comb finger design to keep the capacitor perimeter approximately the same as that of Sensor A despite its smaller wing size. Dimensions of Sensors A and B are listed in Table I, and a photograph of Sensor B is shown in Fig. 8.

According to the estimation made using Eq. (1), the 25 μm thickness of Sensor B should result in a maximum comb finger displacement of about 5 μm. Although detailed measurements of displacement were not done on this sensor, an SEM image, in Fig. 9, shows clearly that the comb fingers are displaced by just a few microns, much less than the device layer thickness.

TABLE I
Sensor Dimensions

	A	B
Vertical thickness of comb fingers t (μm)	10	25
Bridge length (μm)	500	3200
Bridge width (μm)	300	80
Wing area (mm^2)	1.4	2.5
Extent of comb array along wing edge (mm)	4.0	2.6
Combined perimeter of comb fingers l (mm)	104	113
Designed capacitor gap d (μm)	2	2
Comb finger width w (μm)	2	2

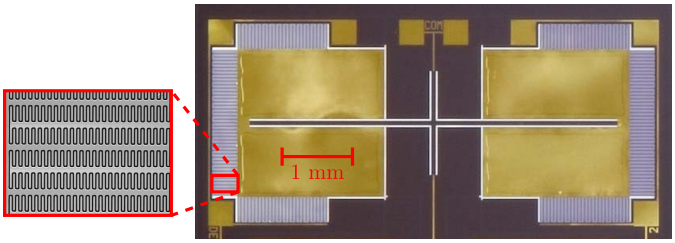

Fig. 8. The sensor with thicker device layer, referred to as Sensor B. The inset shows an SEM image of the branched comb fingers. The scales of image and inset are each the same as the scales in Fig. 1. Gold is deposited onto the wings to increase the mass and lower the resonant frequency.

IV. Results

In order to assess the sensitivity of Sensors A and B to sound, it was necessary to measure their vibration amplitude and electrical output as functions of acoustic driving frequency and pressure. A laser vibrometer was used to measure the sensor's vibration amplitude, and a small microphone was placed near the sensor to measure the sound pressure (see Fig. 10). Finally, a capacitive readout circuit and oscilloscope were connected to the sensor's readout capacitor to measure the electrical output. As mentioned earlier, the readout circuit output voltage varies linearly with changes in capacitance.

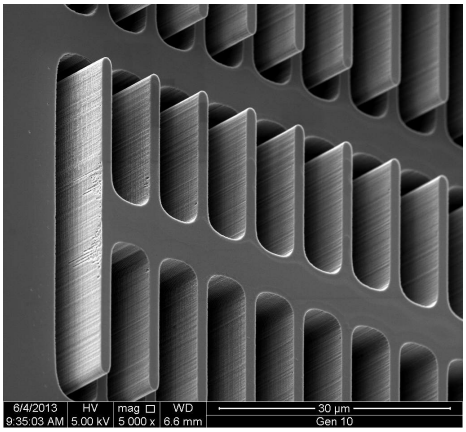

Fig. 9. Sensor B's equilibrium comb finger displacement is much less than the device layer thickness of 25 μm.

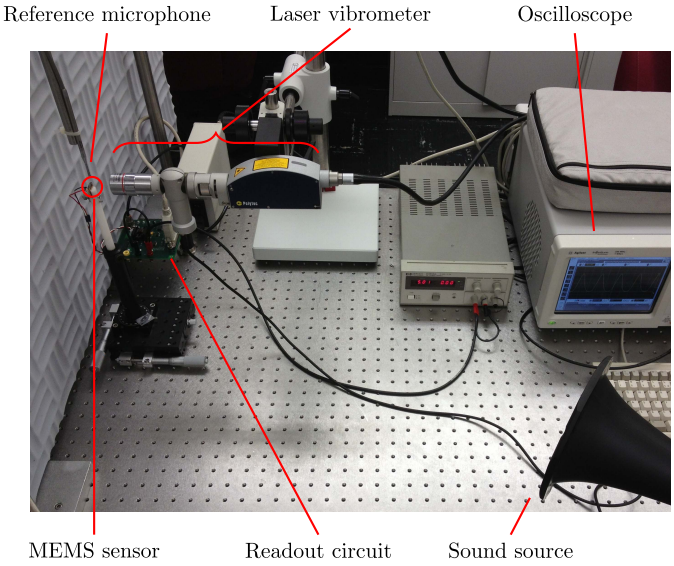

Fig. 10. The experimental setup.

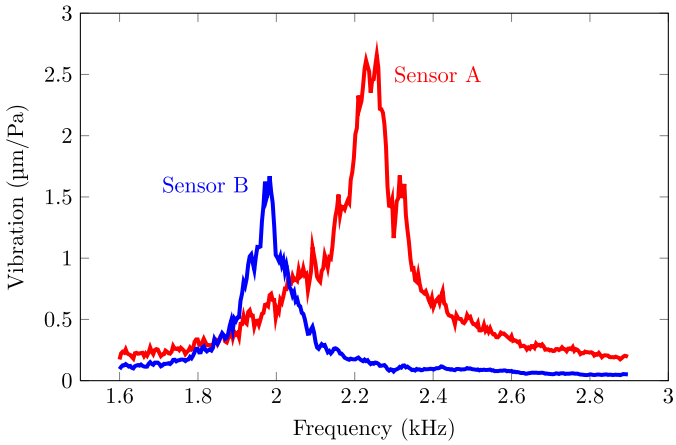

Fig. 11. The vibration transfer functions (μm/Pa) of both sensors as a function of sound frequency.

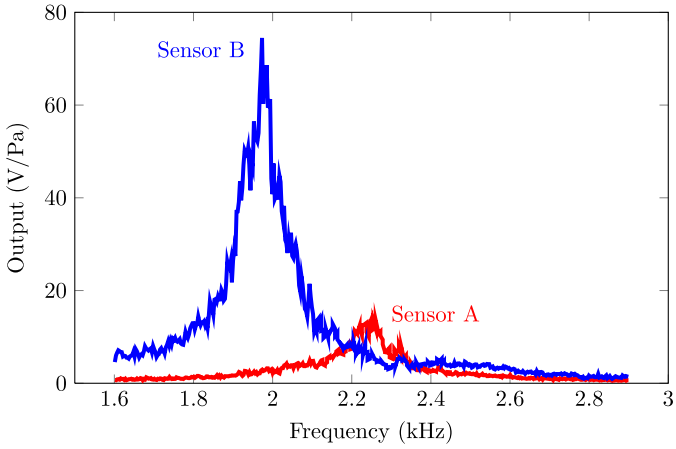

Fig. 12. The electrical output transfer functions (V/Pa) of both sensors as a function of frequency.

Acoustic measurements were conducted in two phases. The first was a frequency sweep, in which the vibration amplitude and electrical output of each sensor were recorded as a function of acoustic driving frequency. This was done by exposing each sensor, separately, to a sound source producing an electronically generated frequency sweep that covered the bending resonance peaks of the two sensors (about 1.5–3 kHz). To negate the effect of inconsistent sound pressure, the measured vibration amplitudes and output voltages were divided by the measured sound pressures. The resulting transfer functions are shown in Fig. 11 and 12. Most of the noise is due to variations in sound pressure with frequency as recorded from the reference microphone.

The vibrational frequency responses in Fig. 11 show a clear resonance peak for each sensor. The peak frequencies are different because of the different sensor dimensions (see Table I). Also, the peak height for Sensor B is smaller due to its greater mass and smaller surface area, which reduces the force due to incident sound pressure. The electrical output as a function of frequency for each sensor is shown in Fig. 12. It can be clearly seen that Sensor B's peak height is several times larger than that of Sensor A despite its smaller vibration amplitude. This result shows that, though the comb finger perimeter is roughly the same in both sensors, the capacitive readout in Sensor B is much more sensitive due to the properly aligned comb fingers.

The next series of measurements probed the linearity of the output voltage over a range of incident acoustic pressure. In this phase of measurements, each sensor was exposed to a sine wave sound source at its resonance peak frequency, and this was repeated at a series of driving acoustic pressures. In each measurement, the vibration amplitude and the output voltage amplitude were recorded at the same time. The sound pressure was measured using the reference microphone placed close to the sensor. These measurements enabled plots of the vibration amplitude as a function of sound pressure, and the output voltage as a function of vibration amplitude, as shown in Fig. 13 and 14.

From Fig. 13, it is evident that in both sensors, the amplitude increases linearly with sound pressure up to at least 2.4 Pa (102 dB), the maximum possible using the available sound source. It is also clear that Sensor A vibrates more readily than Sensor B, as was already seen in the different peak heights in Fig. 11. From Fig. 14, it is clear that the electrical output of

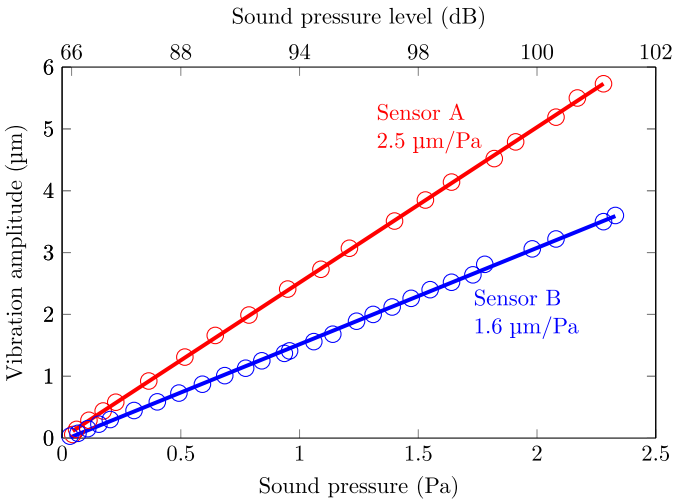

Fig. 13. The vibration amplitude of both sensors as a function of sound pressure, when excited by sound at the resonant frequency.

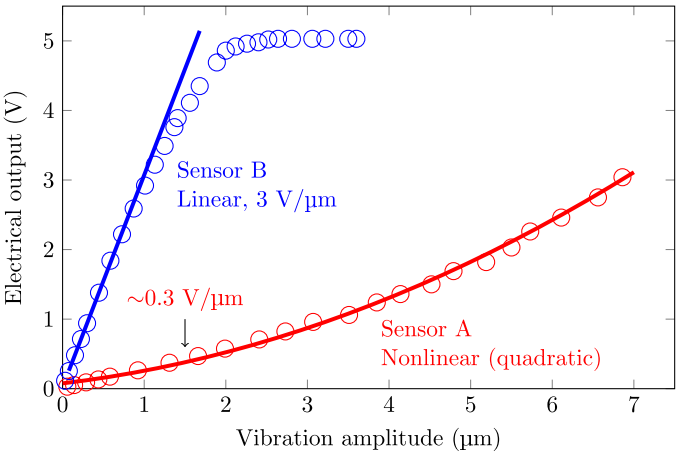

Fig. 14. The electrical output of both sensors as a function of vibration amplitude, when excited by sound at the resonant frequency.

Sensor B is quite linear with vibration amplitude, until the readout circuit begins to saturate approaching the 5 V power supply. The sensitivity, defined as the slope of the line, is 3 V/ μm. For Sensor A, the behavior is more complicated. At low vibration amplitudes, the output voltage increases fairly linearly. However, at higher vibration amplitudes nonlinearity is evident well before the circuit would have saturated. This nonlinearity is due to the comb finger misalignment resulting in capacitance given by Eq. 4.

Eq. 4 can be expanded in a Taylor series around the equilibrium displacement $z = z_0$ to yield

$$\frac{\Delta C(z)}{l} \approx \frac{-\epsilon_0 w}{(z_0 - t)^2}\left[\Delta z + \frac{2(\Delta z)^2}{z_0 - t}\right], \tag{5}$$

where terms of higher order in Δz have been neglected. Based on this form of $\Delta C(z)$, the sensor output should be roughly linear when Δz is small compared to the equilibrium gap $z_0 - t$, but should take on a quadratic form as Δz increases. The red line in Fig. 14 clearly shows the quadratic relationship of the measured output voltage to the vibration amplitude. The 10:1 output ratio seen in Fig. 14 is comparable to the 13:1 output ratio predicted by the FEM.

V. Conclusion

We have presented an enhanced in-plane capacitive readout for sensing out-of-plane displacement in a MEMS acoustic sensor fabricated using the Silicon-On-Insulator Multiuser MEMS Process. It was found that by increasing the device layer thickness, a comb finger misalignment was nearly eliminated. In addition, employing a branched comb design doubled the readout capacitor surface area for a given sensor wing size. These two features combined to restore the linear readout, and to increase the readout sensitivity to vibration by an order of magnitude despite a smaller wing area on the new sensor. The approach described here should be applicable to a variety of MEMS devices that use out-of-plane displacement for sensing.

Acknowledgment

Thanks to B. Kearney for invaluable contributions regarding several aspects of this research, and to N. Haegel for the SEM images.

References

[1] A. Selvakumar and K. Najafi, "A high-sensitivity z-axis capacitive silicon microaccelerometer with a torsional suspension," *J. Microelectromech. Syst.*, vol. 7, no. 2, pp. 192–200, Jun. 1998.

[2] H. Xie and G. Fedder, "Vertical comb-finger capacitive actuation and sensing for CMOS-MEMS," *Sens. Actuators A, Phys.*, vol. 95, nos. 2–3, pp. 212–221, Jan. 2002.

[3] T. Tsuchiya and H. Funabashi, "A z-axis differential capacitive SOI accelerometer with vertical comb," *Sens. Actuators A, Phys.*, vol. 116, no. 3, pp. 378–383, Oct. 2004.

[4] R. N. Miles, D. Robert, and R. R. Hoy, "Mechanically coupled ears for directional hearing in the parasitoid fly *Ormia ochracea*," *J. Acoust. Soc. Amer.*, vol. 98, no. 6, pp. 3059–3070, Dec. 1995.

[5] D. Robert, R. N. Miles, and R. R. Hoy, "Tympanal mechanics in the parasitoid fly *Ormia ochracea*: Intertympanal coupling during mechanical vibration," *J. Comparative Physiol. A*, vol. 183, no. 4, pp. 443–452, 1998.

[6] A. C. Mason, M. L. Oshinsky, and R. R. Hoy, "Hyperacute directional hearing in a microscale auditory system," *Nature*, vol. 410, pp. 686–690, Apr. 2001.

[7] M. Touse, J. Sinibaldi, K. Simsek, J. Catterlin, S. Harrison, and G. Karunasiri, "Fabrication of a microelectromechanical directional sound sensor with electronic readout using comb fingers," *Appl. Phys. Lett.*, vol. 96, no. 17, pp. 173701-1–173701-3, 2010.

[8] R. H. Downey, "Toward a microscale acoustic direction-finding sensor with integrated electronic readout," Ph.D. dissertation, Dept. Phys., Naval Postgraduate School, Monterey, CA, USA, 2013.

[9] R. H. Downey, L. N. Brewer, and G. Karunasiri, "Determination of mechanical properties of a MEMS directional sound sensor using a nanoindenter," *Sens. Actuators A, Phys.*, vol. 191, pp. 27–33, Mar. 2013.

[10] L. E. Kinsler, A. R. Frey, A. B. Coppens, and J. V. Sanders, *Fundamentals of Acoustics*. Hoboken, NJ, USA: Wiley, 2000.

[11] A. Cowen, G. Hames, D. Monk, S. Wilcenski, and B. Hardy, "SOI-MUMPs design handbook: A MUMPs R process," MEMSCAP, Inc., Durham, NC, USA, Tech. Rep. 8.0, 2002.

Richard H. Downey received the B.S. degree in physics from the Massachusetts Institute of Technology, Cambridge, MA, USA, in 1994, the M.S. degree in physics from the University of Illinois at Urbana-Champaign, IL, USA, in 2003, and the Ph.D. degree in applied physics from the Naval Postgraduate School, Monterey, CA, USA, in 2013. His doctoral work consisted of developing MEMS acoustic sensors.

He is an Officer in the U.S. Navy and is currently a faculty member in physics with the U.S. Naval Academy, Annapolis, MD, USA.

Gamani Karunasiri received the Ph.D. degree in physics from the University of Pittsburgh, Pittsburgh, PA, USA, in 1984, and is currently a Professor of physics with the Naval Postgraduate School, Monterey, CA, USA. His current research interests include uncooled terahertz sensors and imaging systems, MEMS-based directional sound sensors and multicolor, and solid state ionizing radiation detectors. He has authored or coauthored over 100 publications in scientific journals.